5074 *Biochemistry* **2009,** *48,* 5074–5082
DOI: 10.1021/bi900345q

BIOCHEMISTRY
including biophysical chemistry & molecular biology
Article

Two Prion Variants of Sup35p Have In-Register Parallel β-Sheet Structures, Independent of Hydration†

Frank Shewmaker,‡ Dmitry Kryndushkin,‡ Bo Chen,§ Robert Tycko,§ and Reed B. Wickner*,‡

‡*Laboratory of Biochemistry and Genetics and* §*Laboratory of Chemical Physics, National Institute of Diabetes and Digestive and Kidney Diseases, National Institutes of Health, Bethesda, Maryland 20892-0830*

Received February 27, 2009; Revised Manuscript Received April 29, 2009

ABSTRACT: The [*PSI*$^+$] prion is a self-propagating amyloid of the Sup35 protein, normally a subunit of the translation termination factor, but impaired in this vital function when in the amyloid form. The Sup35 N, M, and C domains are the amino-terminal prion domain, a connecting polar domain, and the essential C-terminal domain resembling eukaryotic elongation factor 1α respectively. Different [*PSI*$^+$] isolates (prion variants) may have distinct biological properties, associated with different amyloid structures. Here we use solid state NMR to examine the structure of infectious Sup35NM amyloid fibrils of two prion variants. We find that both variants have an in-register parallel β-sheet structure, both in the fully hydrated form and in the lyophilized form. Moreover, we confirm that some leucine residues in the M domain participate in the in-register parallel β-sheet structure. Transmission of the [*PSI*$^+$] prion by amyloid fibrils of Sup35NM and transmission of the [URE3] prion by amyloid fibrils of recombinant full-length Ure2p are similar whether they have been lyophilized or not (wet or dry).

A prion is an infectious protein able to transmit a disease or trait without any essential nucleic acid. This concept arose from studies of the mammalian transmissible spongiform encephalopathies (TSEs), but there are now seven known distinct prions in yeast, [URE3], [*PSI*$^+$], [*PIN*$^+$], [*β*], [*SWI*$^+$], [MCA], and [*OCT*$^+$], based on self-propagating altered forms of Ure2p, Sup35p, Rnq1p, Prb1p, Swi1p, Mca1p, and Cyc8p, respectively (*1*−*6*). Extensive evidence, culminating in transfection by the corresponding amyloid of the recombinant protein, has shown that at least [*PSI*$^+$], [URE3], and [*PIN*$^+$] are based on self-propagating amyloids (*7*−*10*). Amyloid is a fibrillar protein aggregate characterized by partial protease resistance, birefringence on staining with Congo Red, and a cross-β-sheet structure (*11*).

The Sup35 protein is a subunit of the translation termination factor that is inactivated by its aggregation as amyloid in cells infected with the [*PSI* $^+$] prion. The diminished levels of Sup35p lead to inefficient translation termination and thus more frequent read-through of premature termination codons, for example, suppressing a nonsense mutation in *ADE2* and allowing adenine biosynthesis. Sup35p includes an N-terminal 123-residue prion domain (N), whose normal function is in mRNA turnover (*12*), a middle 130-residue charged domain (M), and the C-terminal 432-residue translation termination domain (*13*−*16*). The N domain is both necessary and sufficient for prion propagation (*14*).

A single prion protein sequence can determine several biologically distinguishable infectious entities. In mice, more than a dozen TSE variants are recognized, distinguished by incubation period, distribution of pathology in the brain, species barriers, protease sensitivity of PrP^{Sc}, and glycoform ratios (reviewed in refs *17* and *18*). Variants of the yeast prions [*PSI*$^+$], [URE3], and [*PIN*$^+$] have also been found, distinguished by the intensity of the prion phenotype, stability of prion propagation, response to excess or deficiency of some chaperones, and ability to cross species barriers (*9*, *19*−*25*). Prion variants are a consequence of different amyloid structures which are faithfully propagated (*26*, *27*).

Solid state NMR[1] has been used to study amyloid structure (reviewed in ref *28*), and different amyloids have been found with in-register parallel β-sheet (*29*−*32*), antiparallel β-sheet (*33*, *34*), and parallel β-helix-like (*35*, *36*) structures. Solid state NMR structural studies of infectious amyloid of Sup35NM, $Ure2^{1-89}$, and $Rnq1^{153-405}$ (the prion domains) have indicated that each is an in-register parallel β-sheet, meaning that adjacent peptide chains line up in the same N to C orientation, with corresponding residues opposite each other (Figure 1) (*37*−*39*). The β-sheets are folded along the fibril axis as shown by the diameter of fibrils of the prion domain. Mass per unit length measurements for Ure2p and Sup35p are also consistent with this structure, with each molecule contributing one layer to the fibril (one monomer per 4.7 Å fibril length) (*40*, *41*). The material used in the solid state NMR studies (*37*−*39*) was prepared in a manner known to produce a mixture of prion variants on transfection into yeast

†This work was supported by the Intramural Program of the National Institute of Diabetes and Digestive and Kidney Diseases.

*To whom correspondence should be addressed: Bldg. 8, Room 225, NIH 8 Center Drive, MSC 0830, Bethesda, MD 20892-0830. Phone: (301) 496-3452. Fax: (301) 402-0240. E-mail: wickner@helix.nih.gov.

[1]Abbreviations: CSA, chemical shift anisotropy; NMR, nuclear magnetic resonance; MAS, magic angle spinning.

 Published on Web 05/01/2009

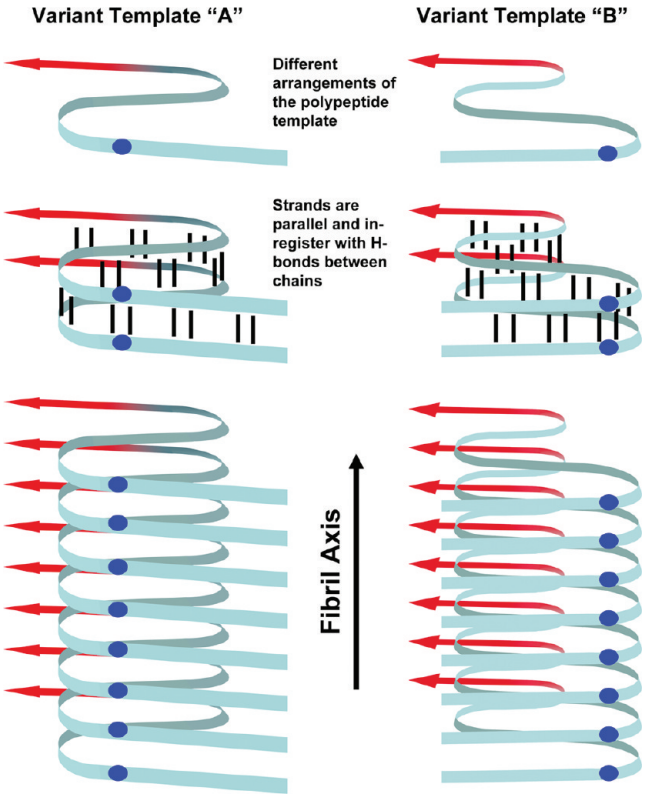

FIGURE 1: Model of in-register parallel β-sheet structure. The yeast prions [PSI^+], [URE3], and [PIN^+] are structurally based on in-register parallel β-sheets. The ribbon represents the prion domain (blue) along with some of the middle domain (red) of Sup35. The prion conformation is propagated through in-register pairing of the polypeptides, thus forming fibrils composed of long parallel β-sheets with the β-strands stacked in a manner perpendicular to the fibril axis. Different prion variants are based on different arrangements of the polypeptide template which are propagated by incorporating free polypeptide into the in-register parallel β-sheets. Residue i of chain n is opposite residue i of the next polypeptide (blue spheres), and hydrogen bonds (black lines) to residues $i \pm 1$ of an adjacent chain are parallel to the fibril axis.

cells (*8*−*10*). Although this was interpreted to mean that the in-register parallel structure is shared by different variants, it is clearly important to verify that this is the case by direct experiments. Weissman's group has found that cells infected with Sup35NM fibrils produced at 4 °C are mostly of a strong variant while those made at 37 °C are nearly all a weak variant (*8*). The 37 °C fibrils are more resistant to heat denaturation and breakage, and show slow H−D exchange extending further toward the C-terminal part of the prion domain than fibrils made at 4 °C (*27*). Here we prepare 37 and 4 °C fibrils, verify the expected phenotypes of their transfectants, and show that both have in-register parallel β-sheet structure.

NMR experiments require relatively large amounts of material packed into a small volume. Lyophilized fibrils are routinely used for this purpose, and previous solid state NMR studies have shown that lyophilization does not perturb the molecular structures of β-amyloid (*34*, *42*) and HETs(218−289) fibrils (*38*). Nonetheless, particularly in light of a previous report that hydrated and lyophilized Sup35NM fibrils may have different X-ray diffraction patterns (*43*), it is important to verify that drying does not perturb the Sup35NM fibril structure. We have therefore analyzed fibrils which have never been dried and find that never-dried fibrils are also in parallel β-sheet structure.

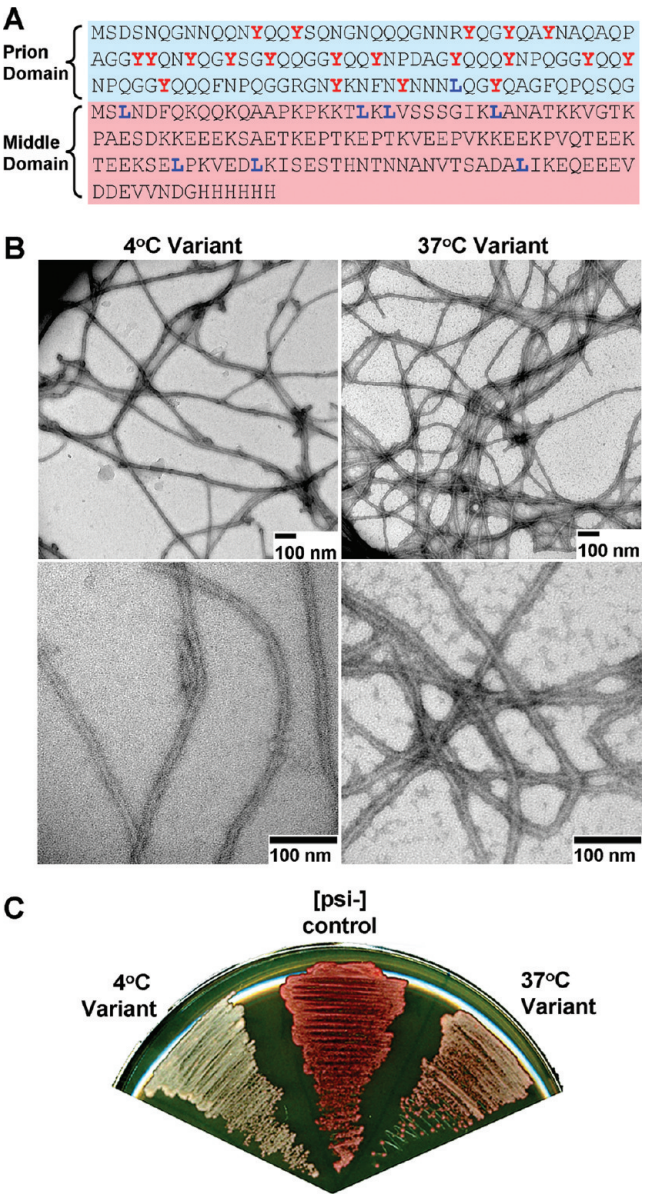

FIGURE 2: Sup35NM amyloid fibrils and prions formed at 4 and 37 °C. (A) All experiments were performed using Sup35NM, which is composed of the prion (N) and middle (M) domains of Sup35 but lacks the C-terminal eRF3 domain. Tyrosine and leucine residues (highlighted in red and blue, respectively) were selectively labeled for NMR experiments. (B) Following purification in denaturant, Sup35NM was exchanged into phosphate buffer at either 4 or 37 °C, whereupon it formed long fibrils. (C) Fibrils formed at both 4 or 37 °C could infect yeast with the [PSI^+] prion following transfection. Fibrils grown at 4 °C conferred a stronger [PSI^+] variant, as reported by whiter yeast colonies on low-adenine medium (see Experimental Procedures).

Importantly, drying does not produce a difference in infectivity for yeast of either Sup35NM or Ure2p fibrils.

EXPERIMENTAL PROCEDURES

Protein Expression and Purification. Sup35NM was expressed from pFPS167, which encodes residues 1−253 with an additional carboxy-terminal histidine tag (see Figure 2A). Freshly transformed BL21-CodonPlus (DE3) RIPL cells with pFPS167 were grown in Defined Amino Acid Medium (DAM) for isotopic labeling using adaptations of established methods (*37*, *44*).

Cells were grown overnight in 50 mL of LB medium with 50 μg/mL ampicillin, 34 μg/mL chloramphenicol, and 100 μg/mL

streptomycin, harvested, and resuspended into 2 L of DAM with 50 μg/mL ampicillin. One liter of DAM contains 100 mL of 10× salts (130 g/L KH_2PO_4, 100 g/L K_2HPO_4, 90 g/L Na_2HPO_4, and 20 g/L NH_4Cl), 10 mL of 100× trace elements [0.6 g of $FeSO_4$, 0.6 g of $CaCl_2$, 0.12 g of $MnCl_2$, 0.08 g of $CoCl_2$, 0.07 g of $ZnSO_4$, 0.03 g of $CuCl_2$, 0.002 g of H_3BO_3, 0.025 g of $(NH_4)_6Mo_7O_{24}$, and 0.5 g of EDTA, all per 100 mL], 10 mL of 100× $MgSO_4$ (1 M), 12 mL of 40% (w/v) glucose, 100 mL of 10× TAU mix (0.3 g/L thiamine, 2 g/L adenine sulfate, and 2 g/L uracil), and 70 mL of AA mix (2 g/L for each amino acid). The cells were grown in DAM at 37 °C with vigorous shaking until they reached an A_{600} of ≈1.0, harvested by centrifugation at ~8000*g* for 7 min, and resuspended in 4 L of prewarmed DAM with the same amino acid composition, except the amino acid with the desired label had been substituted for the unlabeled counterpart at a concentration of 0.2 g/L. After the sample had been shaken for 15 min at 37 °C, protein expression was induced by adding of 1 mM isopropyl β-D-thiogalactopyranoside (IPTG). After ~4 h, the cells were harvested at ~8000*g* and stored at −80 °C or taken directly to the first purification step.

Sup35NM was purified as previously described (*44*). Following protein overexpression, cell pellets were resuspended in 80 mL of 8 M guanidine, 150 mM NaCl, and 100 mM K_2HPO_4 (pH 8) and incubated at room temperature for ~2 h. The cell lysate was cleared by high-speed centrifugation (~150000*g*) for 1 h. The supernatant was mixed with 6 mL of nickel-nitrilotriacetic acid agarose (NiNTA from Qiagen) and incubated at 4 °C for 1 h. The sample and NiNTA were poured into a gravity column and washed twice with 10 mL of 8.5 M urea, 100 mM Na_2HPO_4 (pH 8), 10 mM Tris (pH 8), 150 mM NaCl, and 20 mM imidazole and twice with 10 mL of 8.5 M urea, 10 mM Tris (pH 7.5), 80 mM NaCl, and 20 mM imidazole. The protein was eluted twice with 10 mL of 8.5 M urea, 10 mM Tris (pH 7.5), 80 mM NaCl, and 200 mM imidazole.

The eluate from NiNTA was passed through an equilibrated Q-Sepharose ion exchange column. Following loading, the column was washed with 1 column volume of 8.5 M urea, 10 mM Tris (pH 7.5), and 80 mM NaCl (also used to equilibrate the column). Sup35NM was eluted with an 80 to 160 mM NaCl gradient in the same buffer. The Sup35NM-containing fractions were pooled and dialyzed several times against prewarmed/cooled 5 mM KPO_4 (pH 7.4) and 150 mM NaCl using Pierce dialysis cassettes (20000 molecular weight cutoff). Dialysis was always performed at 4 or 37 °C accordingly. Sup35NM samples were incubated at their respective temperatures for at least 1 week.

Fibrils were harvested by high-speed centrifugation (~150000*g*), which also served to separate fibrils from remaining soluble contaminants. Fibrils were washed several times with water. To achieve very dense samples for solid state NMR, the fibrils were spun at ~280000*g* for 30 min.

Ure2p was expressed from pKT41-1 (*40*), purified by affinity chromatography, and dialyzed against 50 mM sodium phosphate (pH 8.0) and 300 mM NaCl, and fibers formed at room temperature with agitation.

Transfection. Sup35NM fibrils were tested for infectivity by transfection into *Saccharomyces cerevisiae* strain 74-D694 (*MATa ade1-14 ura3 leu2 trp1 his3* [*psi-*]) (*45*) and Ure2p fibrils into *S. cerevisiae* strain DK174 (*MATa kar1 P_{DAL5}ADE2 ura3 trp1 leu2 his3*) as previously described (*9*, *46*).

Electron Microscopy. The formation of Sup35NM fibrils was confirmed by electron microscopy of negatively stained samples. Aqueous suspensions of fibrils were dispensed to carbon-coated copper grids and incubated for several minutes. The fibril suspensions were blotted away; the grids were briefly washed with water, and then 2% uranyl acetate stain was applied to the grids for ~2 min. The stain was blotted away, and the grids were left to air-dry. Fibrils were visualized using an FEI Morgagni transmission electron microscope operating at 80 kV.

Nuclear Magnetic Resonance. Solid state NMR experiments on selectively labeled Sup35NM fibrils were performed at room temperature and 9.39 T (100.4 MHz ^{13}C NMR frequency) using an InfinityPlus spectrometer (Varian, Palo Alto, CA) and magic angle spinning (MAS) NMR probes with 3.2 mm diameter rotors (Varian). ^{13}C NMR spectra were recorded at an MAS frequency of 20 kHz with $^1H-^{13}C$ cross polarization (*47*) and two-pulse phase-modulated decoupling (*48*). PITHIRDS-CT measurements were taken at a MAS frequency of 18 or 20 kHz (*49*), using spin-lock detection for an improved signal-to-noise ratio (*50*). Each PITHIRDS-CT data point is the result of 1024 or more scans with a recyle delay of 4 s.

The raw PITHIRDS-CT data, $S_{raw}(t)$ [where $S_{raw}(0) = 100$], were corrected for the 1.1% natural abundance of ^{13}C based on the roughly linear decay of the signal to 70% of the initial value by 76.8 ms with dry unlabeled samples (*37*). The corrected signal due to the specific label, S_{cor}, was calculated with the equation $S_{cor}(t) = [S_{raw}(t) - f_{na}(100 - 0.39t)]/(1 - f_{na})$, where f_{na} is the fraction of the ^{13}C signal due to natural abundance spins. For dry samples, we assume all natural abundance and specifically labeled carbonyl ^{13}C sites contribute to the signal. For wet samples, we estimate f_{na} assuming that natural abundance carbonyl ^{13}C from all of N and one-third of M contribute to the signal. This estimate is based on our finding that part of the M domain is in β-sheet structure and contributes to the signal but part is not and is presumed to be unstructured (see Results). If all of M were structured, the natural abundance carbonyl ^{13}C correction would increase by one residue equivalent, implying that more leucines are in an in-register parallel β-sheet structure. Thus, this is a conservative assumption. The raw PITHIRDS-CT data are shown in the Supporting Information (Figure S1). Even in the raw data for Leu-1-^{13}C fibrils, it is clear that a significant fraction of the ^{13}C NMR signal decays on the 35 ms time scale typical of in-register parallel β-sheets with 5 Å intermolecular $^{13}C-^{13}C$ distances.

Estimation of Leu Residues in In-Register Parallel β-Sheet Structure. With $N_{0.5}$ being the number of Leu-1-^{13}C residues ~0.5 nm from its nearest Leu-1-^{13}C neighbor and therefore presumably having in-register parallel β sheet structure, S_{iso} is the signal from isolated residues (as in the natural abundance sample), S' is the observed signal from labeled amyloid, $S_{0.5}$ is the simulated signal from a linear array of ^{13}C atoms 4.7 Å apart, and N_{res} is the total number of Leu residues (*8*)

$$N_{0.5} = N_{res}(S_{iso} - S')/(S_{iso} - S_{0.5})$$

That is, the location of the signal between that predicted for 0.5 nm spacing ($S_{0.5}$) and that known for isolated labels (S_{iso}) is assumed to be proportional to the fraction in these forms. For example, if all residues had the 0.5 nm spacing, then S' would equal $S_{0.5}$ and $N_{0.5}$ would equal N_{res}. If all labeled residues were isolated, then S' would equal S_{iso} and $N_{0.5}$ would be zero. Using values at 40 ms for S_{iso} (85 ± 5) and $S_{0.5}$ (23 ± 5), S'_{dry} = 57 ± 5 implies $N_{0.5} = 3.6$, $S'_{wet} = 44$ implies $N_{0.5} = 5.3$, and $S'_{rehydr} = 44$ implies and $N_{0.5} = 5.3$. The increased fraction of Leu-1-^{13}C residues estimated to be within 0.5 nm of their nearest neighbor in wet or rehydrated filaments can be accounted for if

~2.6 Leu residues become mobile in the hydrated state and therefore stop contributing to the solid state NMR signal. The 1.8 remaining Leu residues that contribute to the solid state NMR signal, but whose signals do not decay rapidly in the PITHIRDS-CT measurement, are assumed to be structured, but not in in-register parallel β-sheets.

Two-dimensional $^{1}H-^{13}C$ NMR spectra in Figure 5 were obtained with MAS at 9.5 kHz. $^{1}H-^{13}C$ spin polarization transfer between the t_1 and t_2 dimensions was conducted with a refocused INEPT sequence (*51*), with a total transfer period of 3.4 ms. $^{1}H-^{13}C$ scalar couplings were refocused in the t_1 dimension by a single ^{13}C π pulse at $t_1/2$ and removed in the t_2 dimension by WALTZ decoupling, with a 7.8 kHz ^{1}H rf field.

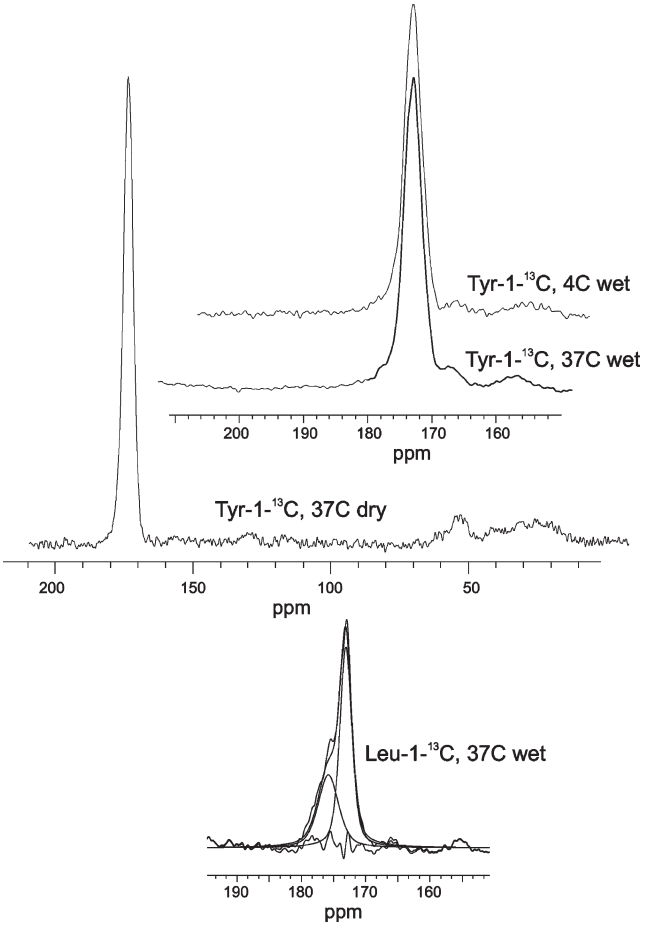

FIGURE 3: One-dimensional solid state NMR spectra. Spectra of Tyr- and Leu-labeled Sup35NM were recorded at 9.39 T using magic angle spinning at 9.0 kHz. The full spectrum of Tyr-1-^{13}C-labeled Sup35NM is shown along with the expanded carbonyl peaks of some of the samples showing the decomposition into major and minor components listed in Table 1.

RESULTS

Sup35NM fibrils were prepared as described previously (*8*) by incubation at either 4 or 37 °C. Although not clearly distinguishable by electron microscopy (Figure 2B), the variants produced on transfection into yeast cells were as described, with a strong [PSI^{+}] variant produced by 4 °C fibrils and a weak variant by 37 °C fibrils (Figure 2C).

The 37 °C Fibrils and 4 °C Fibrils both Have In-Register Parallel β-Sheet Structure. We prepared 4 and 37 °C amyloid fibrils of Sup35NM fully labeled with ^{13}C at the carbonyl position of all tyrosine residues (Figure 2A) and concentrated them by centrifugation but without drying. The one-dimensional spectrum of each (Figure 3) shows a single carbonyl peak at 172.84 ppm with a full width at half-height of ~3 ppm (Table 1). The tyrosine carbonyl ^{13}C frequency expected for random coil residues is 174.2, and residues in a β-sheet conformation are shifted 1−3 ppm to lower values while α-helical residues show shifts to higher values (*33*, *52*−*54*). The tyrosine residues of Sup35NM are distributed throughout the N domain but are absent from the M domain (Figure 2A); this result indicates that all or nearly all are in a β-sheet conformation for amyloids of both prion variants.

The rapid molecular motion of proteins in solution averages out dipole−dipole interactions and chemical shift anisotropies (CSA), but in solid state ^{13}C NMR, MAS is needed to average out dipole−dipole interactions and CSA. Pulse sequences that selectively restore $^{13}C-^{13}C$ dipole−dipole interactions are useful for measuring nearest neighbor distances because the magnitude of the interaction between ^{13}C-labeled atoms is proportional to $1/r^3$. Such pulse sequences are called "dipolar recoupling" sequences. We used the PITHIRDS-CT sequence (*49*), which has been shown to be particularly effective in measurements of relatively large $^{13}C-^{13}C$ distances (>4 Å), even among ^{13}C-labeled sites with large CSA. In PITHIRDS-CT measurements, a train of radio frequency (rf) pulses occupying one-third of each MAS rotation period and rotating the spins of interest by π (thus "PITHIRDS") recouples the dipole−dipole interactions. The effective time of recoupling is varied by shifting certain pulses within the rotation period (*49*), but with a constant total time

Table 1: One-Dimensional Solid State NMR Experiments with Sup35NM[a]

	major components			minor components			
label, hydration	chemical shift (ppm)	line width fwhm (ppm)	fraction	chemical shift (ppm)	line width fwhm (ppm)	fraction	random coil shift (ppm)
37 °C Leu-1-^{13}C dry	173.24	4	0.88	176.45	2.9	0.12	175.9
37 °C Leu-1-^{13}C dry with H_2O	173.29	2.8	0.89	175.8	2.4	0.11	175.9
37 °C Leu-1-^{13}C wet	172.61	2.2	0.59	174.93	2.4	0.25	175.9
				177.14	3.1	0.16	175.9
4 °C Leu-1-^{13}C wet	173.12	2.3	0.58	175.36	1.3	0.42	175.9
37 °C Tyr-1-^{13}C wet	172.84	3.6	1.00				174.2
4 °C Tyr-1-^{13}C wet	172.84	3.3	1.0				174.2
37 °C Tyr-1-^{13}C dry	172.68	4.3	1.0				174.2

[a] The carbonyl peak of each one-dimensional spectrum was fit to a sum of two Gaussian curves. Chemical shifts are relative to tetramethylsilane, and random coil shifts are from Wishart et al. (*58*).

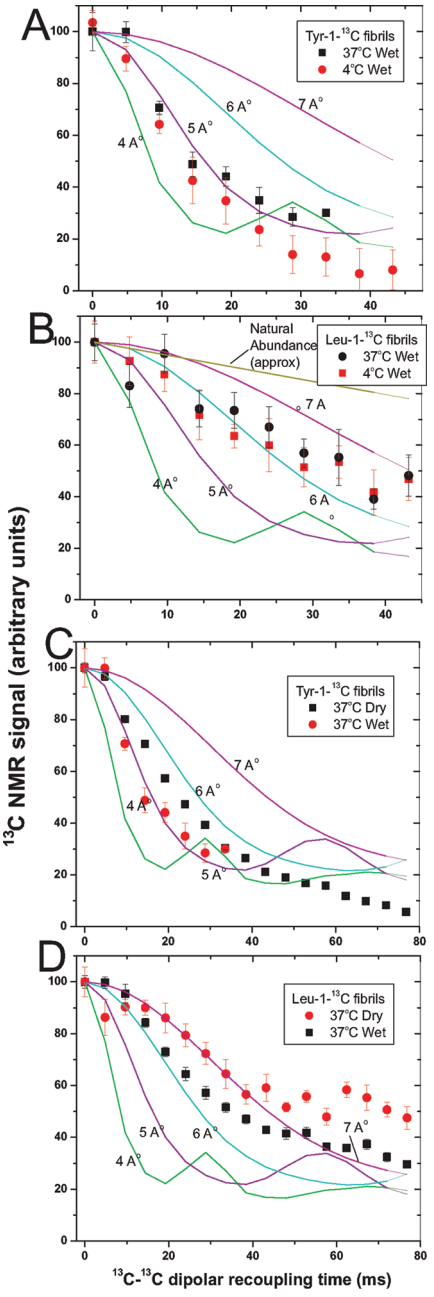

FIGURE 4: Dipolar recoupling experiments. Measurements of $^{13}C-^{13}C$ nuclear magnetic dipole−dipole couplings using the PITHIRDS-CT method at 9.39 T. (A) Comparison of Tyr-1-^{13}C-labeled Sup35NM fibrils formed at 4 or 37 °C using magic angle spinning (MAS) at 18 kHz. Fibrils were compacted by centrifugation but were never dried. Simulated PITHIRDS-CT curves are shown for ideal linear chains of ^{13}C nuclei with the indicated spacings. (B) Comparison of Leu-1-^{13}C-labeled Sup35NM fibrils formed at 4 or 37 °C and never dried. (C) Comparison of Tyr-1-^{13}C-labeled Sup35NM fibrils formed at 37 °C and either never dried (wet) or dried by lyophilization (dry). (D) Comparison of Leu-1-^{13}C-labeled Sup35NM fibrils formed at 37 °C and dried by lyophilization (dry) or rehydrated by addition of water (wet).

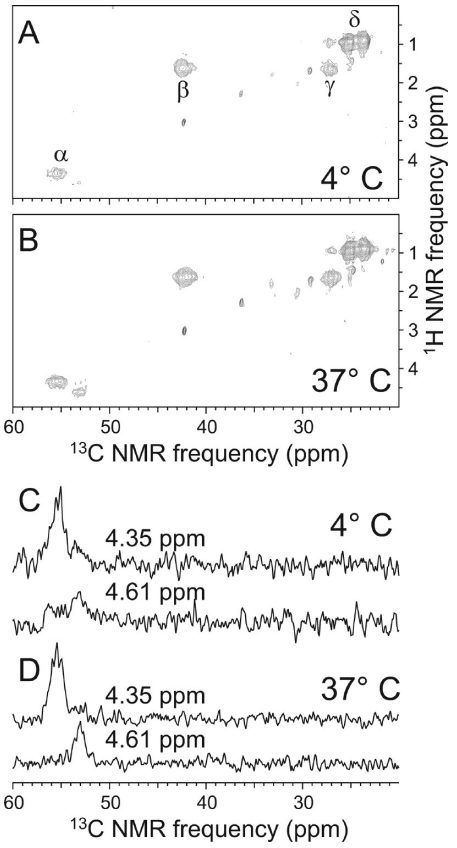

FIGURE 5: Two-dimensional $^{1}H-^{13}C$ NMR spectra. (A and B) Spectra of Sup35NM fibrils formed at 4 and 37 °C, with uniform ^{15}N and ^{13}C labeling of all leucine residues. Spectra were recorded under conditions appropriate for solution NMR, so that only signals from highly mobile residues are observed. Cross-peaks arising from $^{1}H_{\alpha}-^{13}C_{\alpha}$, $^{1}H_{\beta}-^{13}C_{\beta}$, $^{1}H_{\gamma}-^{13}C_{\gamma}$, and $^{1}H_{\delta}-^{13}C_{\delta}$ sites of leucines are indicated. (C and D) One-dimensional slices at ^{1}H chemical shifts of 4.35 and 4.61 ppm, corresponding to major and minor components of the $^{1}H_{\alpha}-^{13}C_{\alpha}$ signals. The minor component is relatively stronger in the spectrum of 37 °C fibrils. Chemical shifts in these spectra are relative to DSS.

before the signal is measured (hence CT = constant time) to minimize effects of T_2 relaxation on the experimental data.

The rate of decay of ^{13}C NMR signals under the PITHIRDS-CT sequence depends on distances among ^{13}C nuclei, as shown by the simulations in Figure 4. Wet (never dried) fibrils of Sup35NM labeled with Tyr-1-^{13}C and formed at 4 °C or at 37 °C each show rates of signal decay indicating a 4.5−5.0 Å distance to the nearest neighbor (Figure 4A), indicating an in-register parallel β-sheet structure as previously shown for fibrils formed at 20 °C (*37*).

The Sup35 M Domain Has Partial β-Sheet Structure in both 4 and 37 °C Filaments. There are eight leucine residues in Sup35NM, only one of which is in the N domain (Figure 2A). Sup35NM Leu-1-^{13}C filaments formed at 4 or 37 °C were examined, without drying, by solid state NMR one-dimensional analysis (Figure 3 and Table 1). The carbonyl peak was best fit by two (or in one case three) Gaussian peaks. The major peak for both samples, accounting for 58% of the signal (~4.6 residues), has a chemical shift of ~173 ppm which is a frequency typical of β-sheet structure.

PITHIRDS-CT experiments with Leu-1-^{13}C filaments, conducted as described for Tyr-1-^{13}C-labeled filaments (above), showed less rapid decay, indicating that not all of the leucine residues had the nearest neighbor $^{13}C-^{13}C$ distances of approximately 5 Å characteristic of in-register parallel β-sheets. Assuming that the signal is a sum of residues in in-register parallel β-sheets and residues outside the β-sheets, with >9 Å nearest neighbor distances, the results can be explained if ~3.6 leucines are in the β-sheets. This result, taken with that for the one-dimensional spectra above, suggests ~4 leucine residues are in in-register parallel β-sheets. The filaments formed at 4 and 37 °C showed nearly the same signal decay rate

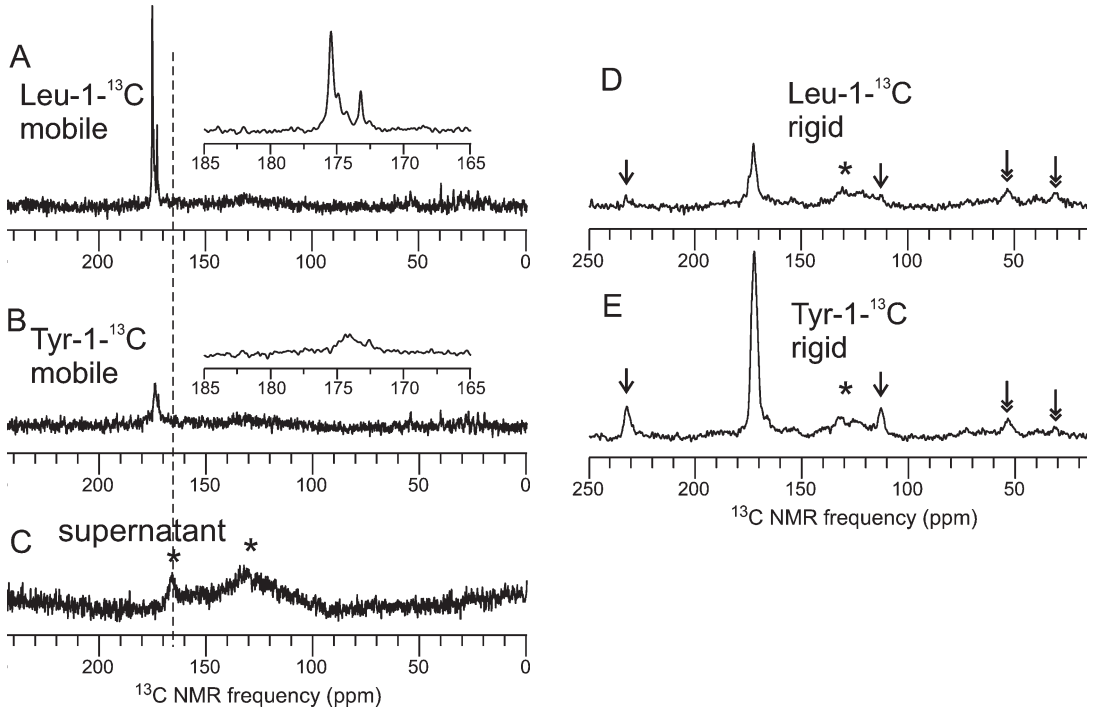

FIGURE 6: Comparisons of solution NMR and solid state NMR spectra. (A) One-dimensional ^{13}C NMR spectrum of Leu-1-^{13}C-labeled Sup35NM fibrils formed at 4 °C, obtained with 512 scans under conditions appropriate for observation of highly mobile protein segments, i.e., direct pulsing of ^{13}C, continuous-wave proton decoupling with a 11 kHz rf field, 6.00 kHz MAS frequency, 2.0 s recycle delay. The inset is an expansion of the carbonyl signal region. The sample was a wet pellet (never dried) in a thin-wall 3.2 mm MAS rotor with a volume of 36 μL, containing 4.6 mg of protein. (B) Same as panel A, but with 4.9 mg of Tyr-1-^{13}C-labeled Sup35NM fibrils formed at 4 °C. All sample and measurement conditions are identical, and the vertical scale is the same as in panel A. (C) Same as panel A, but for the supernatant obtained by suspending the Leu-1-^{13}C-labeled Sup35NM fibril pellet in 50 μL of H_2O and repelleting. The MAS rotor contains 36 μL of supernatant; 16384 scans were acquired, and the vertical scale is reduced by a factor of 4 relative to that in panel A. Asterisks indicate NMR probe background signals at 130 and 165 ppm. (D) Spectrum of Leu-1-^{13}C-labeled Sup35NM fibrils formed at 4 °C (same sample as in panel A), obtained with 2048 scans under conditions appropriate for observation of rigid protein segments, i.e., $^1H-^{13}C$ cross-polarization for 1.5 ms, TPPM proton decoupling with an 85 kHz rf field, a 6.00 kHz MAS frequency, a 2.0 s recycle delay. (E) Same as panel D, but for Tyr-1-^{13}C-labeled Sup35NM fibrils formed at 4 °C (same sample as in panel B). Arrows indicate MAS sideband lines, expected from rigid (but not mobile) carbonyl ^{13}C sites due to their chemical shift anisotropy. Double-headed arrows indicate signals from natural abundance ^{13}C in Sup35NM. The vertical scales in panels D and E are the same. Nearly equal natural abundance signal intensities in panels D and E indicate nearly equal sample quantities.

(Figure 4B), indicating similar numbers of leucine residues in the β-sheets in the two samples.

Sup35NM filaments with uniform ^{15}N and ^{13}C labeling of leucine residues were also grown at 4 and 37 °C. Two-dimensional (2D) $^1H-^{13}C$ NMR spectra of these samples, obtained at room temperature with measurement conditions appropriate for solution NMR rather than solid state NMR [i.e., $^1H-^{13}C$ polarization transfers mediated by scalar couplings rather than dipole−dipole couplings and low ^1H decoupling powers during detection of ^{13}C NMR signals (*55*−*57*)] showed strong cross-peaks at chemical shifts that were within 0.04 and 0.3 ppm (for ^1H and ^{13}C, respectively) of random coil values (*58*) (Figure 5A). The 2D $^1H-^{13}C$ spectra therefore indicate that a subset of the leucine residues (presumably those leucines that are not involved in β-sheet structure) exist in highly mobile segments of the M domain. 2D spectra of 4 and 37 °C filaments were quite similar, although 37 °C filaments exhibited a more intense minority component in the $^1H_\alpha-^{13}C_\alpha$ cross-peak signal (Figure 5B).

It was possible that the NMR signals observed under "solution NMR" conditions arose from Sup35NM molecules in solution, rather than from mobile segments of Sup35NM in fibrils. We thus directly compared ^{13}C NMR spectra of Leu-1-^{13}C-labeled Sup35NM fibrils and Tyr-1-^{13}C-labeled Sup35NM fibrils, both as fully hydrated, never dried, centrifuged pellets. Spectra were obtained both with solution NMR conditions, i.e., direct pulsing of ^{13}C spins and relatively weak proton decoupling (Figure 6A,B), and with "solid state NMR" conditions, i.e., Hartmann−Hahn cross-polarization of ^{13}C spins and relatively strong proton decoupling (Figure 6D,E). The Leu-labeled sample shows strong, sharp carbonyl ^{13}C signals under solution NMR conditions, while the Tyr-labeled sample shows only weaker, broad carbonyl signals under solution NMR conditions. Both samples show carbonyl ^{13}C signals under solid state NMR conditions, but the signals from the Tyr-labeled sample are stronger (but recall that Sup35NM contains 20 Tyr and 8 Leu residues). These results support our claim that the mobile Leu residues are from the fibrils themselves, not from free Sup35NM in solution as the latter possibility would result in mobile Tyr residues as well. In addition, as shown in Figure 6C, we have looked directly for Leu carbonyl signals from free Sup35NM molecules by resuspending and repelleting the fibrils and then recording a ^{13}C NMR spectrum of the supernatant. We see no signals from free Sup35NM, despite extensive signal averaging. Therefore, we conclude that free Sup35NM does not make a measurable contribution to the signals in Figure 6A.

Dried and Never Dried Samples Have Similar Infectivity for Yeast. To address the possibility that drying of protein samples may cause irreversible damage to the structure of amyloid fibrils, we compared the infectivity rates for fibrils with and without drying. In this functional assay, amyloid fibrils were

Table 2: Comparison of Prion Induction by Wet and Dry Amyloid Fibrils[a]

protein	Sup35NM	Ure2p	none (control)
final concentration of wet and dry fibrils (μM)	1.3	0.8	0
conversion to prion, by wet fibrils (%)	31	22	0
conversion to prion, by dry fibrils (%)	31	20	0

[a] Data shown are the average of two experiments. Sup35NM fibrils formed at 4 °C and Ure2p fibrils formed at room temperature were either used without ever having been dried or lyophilized to dryness and rehydrated by addition of water. Fibrils were mixed with pRS425 (LEU2) and introduced into spheroplasts selecting plasmid transformants on Leu with limiting adenine. More than 300 colonies appeared for each fibril type, and tests of Ade+ and curability by guanidine showed the indicated fraction of prion-containing transformants. None of the control plasmid transformants without fibrils were Ade+ and curable.

mixed with plasmid DNA and used to transform non-prion yeast cells by a procedure similar to DNA transformation (*8*, *9*). Together with selection for the DNA plasmid, limited adenine in the medium allowed detection of colonies with a prion induced by the fibrils. In these experiments, freshly formed amyloid fibrils were compared with the same fibrils that underwent drying using conditions that were normally used to prepare samples for solid state NMR experiments. Just before transformation, the dried fibrils were dissolved in water and these rehydrated fibrils as well as wet (never dried) fibrils were sonicated. For these experiments, we used Sup35NM fibrils formed at 4 °C as well as full-length Ure2p fibrils formed at room temperature. The result shown in Table 2 clearly indicates that the infectivity rates of dry and wet fibrils are similar for both proteins, so we conclude that drying of amyloid fibrils before the NMR experiments does not cause an irreversible alteration of their biological effects, consistent with prior evidence that lyophilization does not alter the molecular structures of amyloid fibrils significantly [i.e., NMR chemical shifts of lyophilized and fully hydrated fibrils are the same (*34*, *38*, *42*)].

Solid State NMR of Dried and Never Dried Fibrils. We compared Sup35NM Tyr-1-^{13}C-labeled fibrils made at 37 °C that had been dried by lyophilization, as in our previous report (*37*), or had never been dried (Figure 4C). The wet fibrils exhibited, if anything, a more rapid decay of signal in the PITHIRDS-CT experiment, showing that the in-register parallel structure is not a consequence of drying. The one-dimensional solid state NMR spectrum of wet 37 or 4 °C fibrils each showed a single peak with the shift to lower frequencies indicative of β-sheet structure (Table 1). We previously showed that dry Sup35NM Tyr-1-^{13}C-labeled 20 °C fibrils show a major peak indicating β-sheet (91%) and a minor non-β-sheet peak (9%).

Dry Sup35NM Leu-1-^{13}C-labeled 37 °C fibrils exhibited slower decay in PITHIRDS-CT experiments than did fibrils to which water had been added (Figure 4D), and the one-dimensional spectra showed a higher proportion of β-sheet content. Both results can be explained by loss of some non-β-sheet signal in wet samples; unstructured residues should be mobile in the wet sample and then not contribute to the NMR signal. Note that never dried Sup35NM Leu-1-^{13}C-labeled 37 °C fibrils (Figure 4B) show essentially the same kinetics as those which had been dried and rehydrated (Figure 4D).

DISCUSSION

Prions of yeast or mammals are genes made of protein, in the sense that they carry inherited information and, like genes of DNA or RNA, can even have an array of alleles. The alleles are called "strains" in the mammalian literature and "variants" for yeast prions (to avoid confusion with yeast strains). The molecular basis of prion propagation and prion variants clearly involves self-propagating amyloids differing in structure between variants, but for no variant is the atomic structure yet known. Our earlier work has shown that infectious amyloids of Sup35NM, Ure2p$^{1-89}$, and Rnq1p$^{153-405}$ each have an in-register parallel β-sheet structure (*37*−*39*). Mutations in the N domain affect different prion variants in different ways, suggesting different regions are involved in the β-sheet structure (*59*, *60*). H−D exchange experiments show that fibrils formed at 4 and 37 °C had significantly different distributions of the fastest- and slowest-exchanging components (*27*), indicating significant differences in structure between variant amyloids. In the H−D exchange experiments, most amino acid residues exhibited a mixture of exchange faster than 1 min and exchange slower than 1 week, indicating that although 4 and 37 °C fibrils each include infectious particles producing mostly a single prion variant, the amyloids in each case are significantly heterogeneous.

Our earlier experiments used dried Sup35NM and Ure2$^{1-89}$ fibrils which, in principle, might alter their structure or infectivity. Here, we show that wet and dry fibrils have the same infectivity and that, as previously shown for the dry fibrils, the wet Sup35NM fibrils have an in-register parallel β-sheet structure. Our earlier experiments used infectious fibrils, but those fibrils produced a mixture of prion variants. Here, we prepared fibrils at 4 and 37 °C following Tanaka et al. (*8*) and similarly found that they produced different variants on transfection into yeast. We showed that in both cases the N (prion) domain had in-register parallel β-sheet structure based on data with Tyr-1-^{13}C-labeled fibrils.

We previously estimated that six or seven of the eight Leu residues of Sup35NM fibrils formed at 20 °C were in β-sheets and that all β-sheet Leu residues were in in-register parallel structure (*37*). This indicated that, unexpectedly, the in-register parallel structure extended into the highly charged M domain. These data on wet fibrils formed at 4 or 37 °C yield an estimate of four residues in an in-register parallel β-sheet, consistent with results of Toyama et al. (*27*), both confirming that the in-register parallel β-sheet structure extends into the charged M domain which contains seven of the eight leucines. The different estimates may reflect the different temperatures of sample preparation, a factor shown to be critical in determining structure (*27*).

Of course, an important caveat of all studies of infectious amyloids is that although yeast prion amyloids are highly infectious, the particle/infectious unit ratio must be quite high, so that it is always possible that the physical properties of the bulk of the amyloid are not those of the minority infectious fibrils.

Given that different variants have in-register parallel β-sheet structure, what is the nature of the difference? The ~7−10 nm diameter of Sup35NM fibrils is a fraction of the length of the extended 123-residue N domain (~40 nm), implying that the sheet must be folded several times along the fibril axis. We have previously suggested that variants may differ by the location of the folds or the length of the loops. Moreover, the data of King and of Weissman (*27*, *60*) suggest that the extent of β-sheet structure differs among variants. Differences in the staggering of β-strands in the multilayered structure are also possible (*28*).

The most important feature of our discovery of the in-register parallel β-sheet structure for yeast prions of Sup35p, Ure2p, and Rnq1p is that this structure provides a clear explanation for how variant information is inherited (*39*, *61*, *62*). The end of the fibril

provides a template guiding the conformation assumed by the new monomer joining the fibril to be the same as the last one. The "polar zipper" bonds of Asn and Gln residues (*63*−*65*), possible similar interactions between Ser and Thr residues, and the hydrophobic interactions all favor the in-register parallel structure. Only the repulsion of like-charged residues works against formation of this structure, and such residues are few in number in the prion domains of Sup35p, Ure2p, and Rnq1p.

ACKNOWLEDGMENT

We thank Brian Kimble for help with protein purification and our colleagues for critical reading of the manuscript.

SUPPORTING INFORMATION AVAILABLE

Supplementary Figure 1 shows the PITHIRDS-CT data uncorrected for the signal from natural abundance ^{13}C. This material is available free of charge via the Internet at http://pubs.acs.org.

REFERENCES

1. Wickner, R. B. (1994) [URE3] as an altered *URE2* protein: Evidence for a prion analog in *S. cerevisiae*. *Science 264*, 566–569.
2. Derkatch, I. L., Bradley, M. E., Hong, J. Y., and Liebman, S. W. (2001) Prions affect the appearance of other prions: The story of *[PIN]*. *Cell 106*, 171–182.
3. Roberts, B. T., and Wickner, R. B. (2003) A class of prions that propagate via covalent auto-activation. *Genes Dev. 17*, 2083–2087.
4. Du, Z., Park, K.-W., Yu, H., Fan, Q., and Li, L. (2008) Newly identified prion linked to the chromatin-remodeling factor Swi1 in *Saccharomyces cerevisiae*. *Nat. Genet. 40*, 460–465.
5. Nemecek, J., Nakayashiki, T., and Wickner, R. B. (2009) A prion of yeast metacaspase homolog (Mca1p) detected by a genetic screen. *Proc. Natl. Acad. Sci. U.S.A. 106*, 1892–1896.
6. Patel, B. K., Gavin-Smyth, J., and Liebman, S. W. (2009) The yeast global transcriptional co-repressor protein Cyc8 can propagate as a prion. *Nat. Cell Biol. 11*, 344–349.
7. King, C. Y., and Diaz-Avalos, R. (2004) Protein-only transmission of three yeast prion strains. *Nature 428*, 319–323.
8. Tanaka, M., Chien, P., Naber, N., Cooke, R., and Weissman, J. S. (2004) Conformational variations in an infectious protein determine prion strain differences. *Nature 428*, 323–328.
9. Brachmann, A., Baxa, U., and Wickner, R. B. (2005) Prion generation *in vitro*: Amyloid of Ure2p is infectious. *EMBO J. 24*, 3082–3092.
10. Patel, B. K., and Liebman, S. W. (2007) "Prion proof" for [PIN+]: Infection with in vitro-made amyloid aggregates of Rnq1p-(132−405) induces [PIN+]. *J. Mol. Biol. 365*, 773–782.
11. Sipe, J. D. (1992) Amyloidosis. *Annu. Rev. Biochem. 61*, 947–975.
12. Hosoda, N., Kobayashii, T., Uchida, N., Funakoshi, Y., Kikuchi, Y., Hoshino, S., and Katada, T. (2003) Translation termination factor eRF3 mediates mRNA decay through the regulation of deadenylation. *J. Biol. Chem. 278*, 38287–38291.
13. Wilson, P. G., and Culbertson, M. R. (1988) *SUF12* suppressor protein of yeast: A fusion protein related to the EF-1 family of elongation factors. *J. Mol. Biol. 199*, 559–573.
14. TerAvanesyan, A., Dagkesamanskaya, A. R., Kushnirov, V. V., and Smirnov, V. N. (1994) The *SUP35* omnipotent suppressor gene is involved in the maintenance of the non-Mendelian determinant [psi+] in the yeast *Saccharomyces cerevisiae*. *Genetics 137*, 671–676.
15. Frolova, L., LeGoff, X., Rasmussen, H. H., Cheperegin, S., Drugeon, G., Kress, M., Arman, I., Haenni, A.-L., Celis, J. E., Philippe, M., Justesen, J., and Kisselev, L. (1994) A highly conserved eukaryotic protein family possessing properties of polypeptide chain release factor. *Nature 372*, 701–703.
16. Stansfield, I., Jones, K. M., Kushnirov, V. V., Dagkesamanskaya, A. R., Poznyakovski, A. I., Paushkin, S. V., Nierras, C. R., Cox, B. S., Ter-Avanesyan, M. D., and Tuite, M. F. (1995) The products of the *SUP45* (eRF1) and *SUP35* genes interact to mediate translation termination in *Saccharomyces cerevisiae*. *EMBO J. 14*, 4365–4373.
17. Bruce, M. E. (1993) Scrapie strain variation and mutation. *Br. Med. Bull. 49*, 822–838.
18. Collinge, J., and Clarke, A. R. (2007) A general model of prion strains and their pathogenicity. *Science 318*, 930–936.
19. Derkatch, I. L., Chernoff, Y. O., Kushnirov, V. V., Inge-Vechtomov, S. G., and Liebman, S. W. (1996) Genesis and variability of [*PSI*] prion factors in *Saccharomyces cerevisiae*. *Genetics 144*, 1375–1386.
20. Schlumpberger, M., Prusiner, S. B., and Herskowitz, I. (2001) Induction of distinct [URE3] yeast prion strains. *Mol. Cell. Biol. 21*, 7035–7046.
21. Bradley, M. E., Edskes, H. K., Hong, J. Y., Wickner, R. B., and Liebman, S. W. (2002) Interactions among prions and prion "strains" in yeast. *Proc. Natl. Acad. Sci. U.S.A. 99* (Suppl. 4), 16392–16399.
22. Kryndushkin, D., and Wickner, R. B. (2007) Nucleotide exchange factors for Hsp70s are required for [URE3] prion propagation in *Saccharomyces cerevisiae*. *Mol. Biol. Cell 18*, 2149–2154.
23. Kryndushkin, D., Shewmaker, F., and Wickner, R. B. (2008) Curing of the [URE3] prion by Btn2p, a Batten disease-related protein. *EMBO J. 27*, 2725–2735.
24. Kushnirov, V. V., Kryndushkin, D., Boguta, M., Smirnov, V. N., and Ter-Avanesyan, M. D. (2000) Chaperones that cure yeast artificial [PSI^+] and their prion-specific effects. *Curr. Biol. 10*, 1443–1446.
25. Edskes, H. K., McCann, L. M., Hebert, A. M., and Wickner, R. B. (2009) Prion variants and species barriers among *Saccharomyces* Ure2 proteins. *Genetics 181*, 1159–1167.
26. Bessen, R. A., and Marsh, R. F. (1994) Distinct PrP properties suggest the molecular basis of strain variation in transmissible mink encephalopathy. *J. Virol. 68*, 7859–7868.
27. Toyama, B. H., Kelly, M. J., Gross, J. D., and Weissman, J. S. (2007) The structural basis of yeast prion strain variants. *Nature 449*, 233–237.
28. Tycko, R. (2006) Molecular structure of amyloid fibrils: Insights from solid-state NMR. *Q. Rev. Biophys. 1*, 1–55.
29. Benzinger, T. L., Gregory, D. M., Burkoth, T. S., Miller-Auer, H., Lynn, D. G., Botto, R. E., and Meredith, S. C. (1998) Propagating structure of Alzheimer's β-amyloid(10−35) is parallel β-sheet with residues in exact register. *Proc. Natl. Acad. Sci. U.S.A. 95*, 13407–13412.
30. Antzutkin, O. N., Balbach, J. J., Leapman, R. D., Rizzo, N. W., Reed, J., and Tycko, R. (2000) Multiple quantum solid-state NMR indicates a parallel, not antiparallel, organization of β-sheets in Alzheimer's β-amyloid fibrils. *Proc. Natl. Acad. Sci. U.S.A. 97*, 13045–13050.
31. Balbach, J. J., Petkova, A. T., Oyler, N. A., Antzutkin, O. N., Gordon, D. J., Meredith, S. C., and Tycko, R. (2002) Supramolecular structure in full-length Alzheimer's β-amyloid fibrils: Evidence for a parallel β-sheet organization from solid-state nuclear magnetic resonance. *Biophys. J. 83*, 1205–1216.
32. Jaroniec, C. P., MacPhee, C. E., Bajaj, V. S., McMahon, M. T., Dobson, C. M., and Griffin, R. G. (2004) High-resolution molecular structure of a peptide in an amyloid fibril determined by magic angle spinning NMR spectroscopy. *Proc. Natl. Acad. Sci. U.S.A. 101*, 711–716.
33. Balbach, J. J., Ishii, Y., Antzutkin, O. N., Leapman, R. D., Rizzo, N. W., Dyda, F., Reed, J., and Tycko, R. (2000) Amyloid fibril formation by Aβ 16−22, a seven-residue fragment of the Alzheimer's β-amyloid peptide, and structural characterization by solid state NMR. *Biochemistry 39*, 13748–13759.
34. Petkova, A. T., Buntkowsky, G., Dyda, F., Leapman, R. D., Yau, W. M., and Tycko, R. (2004) Solid state NMR reveals a pH-dependent antiparallel β-sheet registry in fibrils formed by a β-amyloid peptide. *J. Mol. Biol. 335*, 247–260.
35. Ritter, C., Maddelein, M. L., Siemer, A. B., Luhrs, T., Ernst, M., Meier, B. H., Saupe, S. J., and Riek, R. (2005) Correlation of structural elements and infectivity of the HET-s prion. *Nature 435*, 844–848.
36. Wasmer, C., Lange, A., Van Melckebeke, H., Siemer, A. B., Riek, R., and Meier, B. H. (2008) Amyloid fibrils of the HET-s(218−279) prion form a β solenoid with a triangular hydrophobic core. *Science 319*, 1523–1526.
37. Shewmaker, F., Wickner, R. B., and Tycko, R. (2006) Amyloid of the prion domain of Sup35p has an in-register parallel β-sheet structure. *Proc. Natl. Acad. Sci. U.S.A. 103*, 19754–19759.
38. Baxa, U., Wickner, R. B., Steven, A. C., Anderson, D., Marekov, L., Yau, W.-M., and Tycko, R. (2007) Characterization of β-sheet structure in Ure2p1−89 yeast prion fibrils by solid state nuclear magnetic resonance. *Biochemistry 46*, 13149–13162.
39. Wickner, R. B., Dyda, F., and Tycko, R. (2008) Amyloid of Rnq1p, the basis of the [PIN^+] prion, has a parallel in-register β-sheet structure. *Proc. Natl. Acad. Sci. U.S.A. 105*, 2403–2408.
40. Baxa, U., Taylor, K. L., Wall, J. S., Simon, M. N., Cheng, N., Wickner, R. B., and Steven, A. (2003) Architecture of Ure2p prion filaments: The N-terminal domain forms a central core fiber. *J. Biol. Chem. 278*, 43717–43727.
41. Diaz-Avalos, R., King, C. Y., Wall, J. S., Simon, M., and Caspar, D. L. D. (2005) Strain-specific morphologies of yeast prion amyloids. *Proc. Natl. Acad. Sci. U.S.A. 102*, 10165–10170.

42. Paravastu, A. K., Petkova, A. T., and Tycko, R. (2006) Polymorphic fibril formation by residues 10−40 of the Alzheimer's β-amyloid polypeptide. *Biophys. J. 90*, 4618–4629.
43. Kishimoto, A., Hasegawa, K., Suzuki, H., Taguchi, H., Namba, K., and Yoshida, M. (2004) β-Helix is a likely core structure of yeast prion Sup35 amyloid fibers. *Biochem. Biophys. Res. Commun. 315*, 739–745.
44. Shewmaker, F., Ross, E. D., Tycko, R., and Wickner, R. B. (2008) Amyloids of shuffled prion domains that form prions have a parallel in-register β-sheet structure. *Biochemistry 47*, 4000–4007.
45. Chernoff, Y. O., Lindquist, S. L., Ono, B.-I., Inge-Vechtomov, S. G., and Liebman, S. W. (1995) Role of the chaperone protein Hsp104 in propagation of the yeast prion-like factor [psi$^+$]. *Science 268*, 880–884.
46. Brachmann, A., Toombs, J. A., and Ross, E. D. (2006) Reporter assay systems for [URE3] detection and analysis. *Methods 39*, 35–42.
47. Pines, A., Gibby, M. G., and Waugh, J. S. (1973) Proton-Enhanced Nmr of Dilute Spins in Solids. *J. Chem. Phys. 59*, 569–590.
48. Bennett, A. E., Rienstra, C. M., Auger, M., Lakshmi, K. V., and Griffin, R. G. (1995) Heteronuclear Decoupling in Rotating Solids. *J. Chem. Phys. 103*, 6951–6958.
49. Tycko, R. (2007) Symmetry-based constant-time homonuclear dipolar recoupling in solid-state NMR. *J. Chem. Phys. 126*, 064506.
50. Petkova, A. T., and Tycko, R. (2002) Sensitivity enhancement in structural measurements by solid state NMR through pulsed spin locking. *J. Magn. Reson. 155*, 293–299.
51. Morris, G. A., and Freeman, R. (1979) Enhancement of nuclear magnetic resonance signals by polarization transfer. *J. Am. Chem. Soc. 101*, 760–762.
52. Wishart, D. S., Sykes, B. D., and Richards, F. M. (1991) Relationship between nuclear magnetic resonance chemical shift and protein secondary structure. *J. Mol. Biol. 222*, 311–333.
53. Petkova, A. T., Ishii, Y., Balbach, J. J., Antzutkin, O. N., Leapman, R. D., Delaglio, F., and Tycko, R. (2002) A structural model for Alzheimer's β-amyloid fibrils based on experimental constraints from solid state NMR. *Proc. Natl. Acad. Sci. U.S.A. 99*, 16742–16747.
54. Petkova, A. T., Leapman, R. D., Guo, Z., Yau, W. M., Mattson, M. P., and Tycko, R. (2005) Self-propagating, molecular-level polymorphism in Alzheimer's β-amyloid fibrils. *Science 307*, 262–265.
55. Heise, H., Hoyer, W., Becker, S., Andronesi, O. C., Riedel, D., and Baldus, M. (2005) Molecular-level secondary structure, polymorphism, and dynamics of full-length α-synuclein fibrils studied by solid-state NMR. *Proc. Natl. Acad. Sci. U.S.A. 102*, 15871–15876.
56. Andronesi, O. C., Becker, S., Seidel, K., Heise, H., Young, H. S., and Baldus, M. (2005) Determination of membrane protein structure and dynamics by magic-angle-spinning solid-state NMR spectroscopy. *J. Am. Chem. Soc. 127*, 12965–12974.
57. Siemer, A. B., Arnold, A. A., Ritter, C., Westfeld, T., Ernst, M., Riek, R., and Meier, B. H. (2006) Observation of highly flexible residues in amyloid fibrils of the HET-s prion. *J. Am. Chem. Soc. 128*, 13224–13228.
58. Wishart, D. S., Bigam, C. G., Holm, A., Hodges, R. S., and Sykes, B. D. (1995) H-1, C-13 and N-15 Random Coil NMR Chemical-Shifts of the Common Amino-Acids 0.1. Investigations of Nearest-Neighbor Effects. *J. Biomol. NMR 5*, 67–81.
59. King, C. Y. (2001) Supporting the structural basis of prion strains: Induction and identification of [*PSI*] variants. *J. Mol. Biol. 307*, 1247–1260.
60. Chang, H.-Y., Lin, J.-Y., Lee, H.-C., Wang, H.-L., and King, C.-Y. (2008) Strain-specific sequences required for yeast prion [PSI+] propagation. *Proc. Natl. Acad. Sci. U.S.A. 105*, 13345–13350.
61. Ross, E. D., Minton, A. P., and Wickner, R. B. (2005) Prion domains: Sequences, structures and interactions. *Nat. Cell Biol. 7*, 1039–1044.
62. Wickner, R. B., Shewmaker, F., Kryndushkin, D., and Edskes, H. K. (2008) Protein inheritance (prions) based on parallel in-register β-sheet amyloid structures. *BioEssays 30*, 955–964.
63. Perutz, M. F., Johnson, T., Suzuki, M., and Finch, J. T. (1994) Glutamine repeats as polar zippers: Their possible role in inherited neurodegenerative diseases. *Proc. Natl. Acad. Sci. U.S.A. 91*, 5355–5358.
64. Chan, J. C. C., Oyler, N. A., Yau, W.-M., and Tycko, R. (2005) Parallel β-sheets and polar zippers in amyloid fibrils formed by residues 10−39 of the yeast prion protein Ure2p. *Biochemistry 44*, 10669–10680.
65. Nelson, R., Sawaya, M. R., Balbirnie, M., Madsen, A. O., Riekel, C., Grothe, R., and Eisenberg, D. (2005) Structure of the cross-β spine of amyloid-like fibrils. *Nature 435*, 773–778.